BULLETIN OF STOMATOLOGY AND MAXILLOFACIAL SURGERY
Volume 21, Issue 7

DOI: 10.58240/1829006X-2025.21.7-290

ORIGINAL ARTICLE

OSTEOGENIC POTENTIAL OF A NOVEL EU_2O_3 /AG_2O/SRO-ADDED COLLAGEN– CHITOSAN MEMBRANE FOR PERIODONTAL REGENERATION: AN IN VITRO STUDY

REENU JOSHY[1], NIDHITA SURESH[2], KAARTHIKEYAN GURUMOORTHY[3], SUBRAMANIAN RAGHUNANDHAKUMAR[4]

[1]Department of Periodontics,Saveetha Dental college,SaveethaInstitute of Medical and Technical Sciences,Saveetha University 162,Poonamallee High Road, Chennai, India, Email ID: 152001030.sdc@saveetha.com.

[2]M.D.S, Assistant Professor, Department Of Periodontics, Saveetha dental college, Saveetha Institute Of Medical And Technical Sciences, Saveetha University 162,Poonamallee High Road, Chennai, India, Email ID:drnidhitasuresh@gmail.com.

[3.]M.D.S, Phd , Department Of Periodontics, Saveetha dental college, Saveetha Institute Of Medical And Technical Sciences, Saveetha University 162,Poonamallee High Road, Chennai, India, Email ID: kaarthikeyan@saveetha.com.

[4.]Department of Pharmacology,Saveetha dental college, Saveetha Institute Of Medical And Technical Sciences, Saveetha University 162,Poonamallee High Road, Chennai, India, Email ID- raghunandhakumar@gmail.com

Corresponding author* Dr.Nidhita Suresh Assistant Professor, Department of Periodontics Institution Name: Saveetha dental college, Saveetha Institute Of Medical And Technical Sciences, Saveetha University 162,Poonamallee High Road, Chennai, India Orchid ID- https://orcid.org/0009-0008-4528-4541 Email ID-drnidhitasuresh@gmail.com.

Received:*Jun.28 2025;* ***Accepted:*** *Jul 29, 2025;* ***Published:*** *Aug 15.2025*

Background: Guided tissue regeneration (GTR) plays a critical role in periodontal therapy, but conventional membranes often exhibit limited bioactivity and may induce inflammatory responses, thereby impairing effective bone regeneration. This study aims to develop and evaluate a resorbable collagen–chitosan membrane enriched with Eu_2O_3 , Ag_2O, and SrO, based on the hypothesis that the incorporation of these bioactive components enhances osteogenic potential, antioxidant activity, and cytocompatibility.

Methods: A novel collagen–chitosan membrane containing Eu_2O_3 , Ag_2O, and SrO was synthesized and characterized. The antioxidant activity was measured using the DPPH assay. Cytocompatibility was assessed via MTT assays and fluorescence microscopy using human periodontal ligament stem cells (PDLSCs) and osteoblasts. Osteogenic differentiation was assessed by quantifying BMP-2 and ALP gene expression using real-time PCR at days 1, 7, 14, and 21. Comparative evaluation was conducted against PerioCol GTR and strontium/silver-doped collagen–chitosan membranes. Statistical significance was set at $p < 0.05$.

Results: The Eu_2O_3 /Ag_2O/SrO-enriched membrane exhibited significantly enhanced antioxidant activity, comparable to that ofascorbic acid. MTT assays indicated high cell viability, while fluorescence microscopy demonstrated increased cell proliferation on days 3 and 5. Gene expression analysis revealed significantly elevated BMP-2 and ALP mRNA levels ($p < 0.05$) in the europium-doped group, with peak expression observed at day 14, suggesting enhanced osteogenic differentiation.

Conclusion: Propofol and sevoflurane showed superior efficacy but require specialized monitoring. Nitrous oxide and midazolam remain safe first-line options despite moderate success rates. The choice of sedation technique should consider patient factors, procedure complexity, and available expertise. Further research is needed to optimize sedation protocols and minimize adverse events.

Keywords: Guided tissue regeneration, Rare earth element, Europium, Periodontal regeneration

INTRODUCTION

The healthy periodontium is a complex unit consisting of several structural components-such as the gingiva, periodontal ligament, cementum, and alveolar bone-each playing a vital role. The coordinated interaction among these tissues and their cellular and molecular constituents is essential for maintaining oral health.
However, pathological conditions, such as periodontitis, disrupt this structure, leading to tooth loss and alveolar bone resorption [1]. Effective management of periodontal defects requires both conventional and regenerative therapeutic strategies. Among these, GTR has emerged as a pivotal approach due to its ability to selectively promote the growth of periodontal-supporting tissues while excluding undesirable cellular invasion.[2-4]
Originally introduced by Hurley in the 1950s for spinal bone regeneration [5], the GTR concept was later adapted in the 1980s for periodontal applications.[6] The technique involves the placement of a barrier membrane that prevents rapid epithelial and connective tissue cell migration into the periodontal defect, thereby allowing slower-growing cells, such as those from the periodontal ligament, cementum, and alveolar bone, to repopulate the site.[7-8]

An ideal GTR membrane must be biocompatible, space maintaining, cell occlusive, integrative with host tissue, and clinically manageable.[9] Membranes have traditionally been categorized into non-resorbable and bioresorbable types. First-generation non-resorbable membranes, though effective, required secondary surgical removal. In contrast, second-generation bioresorbable membranes eliminated this drawback through the use of natural or synthetic biodegradable polymers.[5]Despite these advancements, many current GTR membranes suffer from limitations such as suboptimal biocompatibility, poor mechanical properties, limited antimicrobial efficacy, and lack of active biological stimulation, which collectively compromise GTR's regenerative potential and clinical success.[10]

To address these challenges, composite membranes, which are membranes combined with natural polymers such as collagen and chitosan, have been explored. Collagen, a major extracellular matrix protein, promotes cellular adhesion, migration, and differentiation . [11-13] Chitosan, which is derived from chitin, offers biocompatibility, biodegradability, and antimicrobial effects. Its resemblance to glycosaminoglycans enhances its compatibility in dental applications. However, chitosan's poor mechanical integrity, low hydrophilicity, and weak mineral-binding capacity restrict its standalone performance in mineralized tissue regeneration.[14-17] Integrating collagen with chitosan improves the mechanical and biological profile of the membrane, thus providing a more favourable microenvironment for tissue regeneration.

The regenerative capacity of such composite scaffolds is further enhanced by doping with bioactive elements. Strontium has been shown to stimulate osteoblast activity and inhibit bone resorption, with additional roles in activating ERK1/2-MAPK signalling, modulating immune responses, and promoting angiogenesis via VEGF and PI3K/AKT/mTOR pathways.[18-20] Europium, a lanthanide element, enhances osteogenic differentiation, angiogenesis, and mineralization. Its intrinsic fluorescence enables non-invasive imaging of tissue regeneration and scaffold degradation—an attribute not commonly available in standard GTR membranes.[21-23] Silver nanoparticles contribute potent antibacterial effects and stimulate tissue healing via fibroblast activation, collagen synthesis, and modulation of TGF-β/BMP signalling .[24,25]

Although several collagen- and chitosan-based GTR membranes have been developed, a significant research gap remains in designing multifunctional bioresorbable membranes that simultaneously provide osteogenic stimulation, antimicrobial activity, and real-time imaging capabilities. Existing commercial membranes, such as Periocol, primarily serve as passive barriers without actively enhancing tissue regeneration or offering diagnostic advantages.

To address these limitations, the present study focuses on the development of a resorbable $Eu_2 O_3$ /$Ag_2 O$/SrO-added collagen–chitosan membrane and evaluates its antioxidant properties, biocompatibility, and osteogenic potential using human PDLSCs and osteoblasts. The novelty of this work lies in the synergistic integration of bioactivity and imaging potential within a single biodegradable scaffold, representing a next-generation GTR membrane with enhanced regenerative functionality. These findings provide important insights into the clinical translation of advanced biocomposite materials for improved periodontal regeneration outcomes.

MATERIALS AND METHODS

The $Eu_2 O_3$ /$Ag_2 O$/SrO-doped collagen–chitosan membrane was prepared using a stepwise approach to ensure uniform distribution of bioactive components. First, 3 g of chitosan were dissolved in 100 mL of distilled water to create a 3% (w/v) chitosan solution. Simultaneously, a 1% (w/v) collagen solution was prepared by dissolving 0.15 g of collagen in 15 mL of distilled water. To facilitate cross-linking and enhance membrane stability, 0.5 g of succinic acid was added to the chitosan solution. The cross-linking process was further optimized by incorporating 0.5664 g of 3-dimethylaminopropyl carbodiimide (EDC) and 0.33923 g of *N*-hydroxysuccinimide (NHS) to activate the carboxyl groups and improve polymer network formation. For bioactivity enhancement and fluorescent tracking, 0.01mol of europium ions (Eu^{3+}) were introduced into the chitosan solution, ensuring homogeneous dispersion within the polymer matrix. Meanwhile, silver and strontium nanoparticles were prepared separately, with 2.5 g of silver nanoparticles and 5 g of strontium nanoparticles, which were then mixed into the collagen solution to ensure uniform distribution. The europium-enriched chitosan solution and the silver/strontium-enriched collagen solution were then combined under continuous stirring to achieve thorough integration of all bioactive components. The final mixture was frozen at -80°C overnight to preserve the structural integrity of the polymeric network. Subsequently, it was subjected to lyophilization (freeze-drying) for 24 h, resulting in the formation of a porous, resorbable membrane with enhanced bioactivity, osteogenic potential, and antimicrobial properties.[26]

The membrane's biocompatibility and cycompatibility were evaluated by culturing human PDLSCs and osteoblasts on the membrane surfaces.

Cell viability and proliferation were assessed using the MTT assay, and cell attachment was observed using live/dead staining. Additionally, the osteogenic potential of the membrane was evaluated by analysing the temporal mRNA expression of osteogenic markers, including ALP and bone morphogenetic protein-2 (BMP-2), using qPCR. These analyses provided insights into the membrane's ability to support periodontal tissue regeneration. The overall experimental workflow of this in vitro study, including membrane fabrication, characterization, and biological evaluation, is summarized in the flowchart (Figure 1).

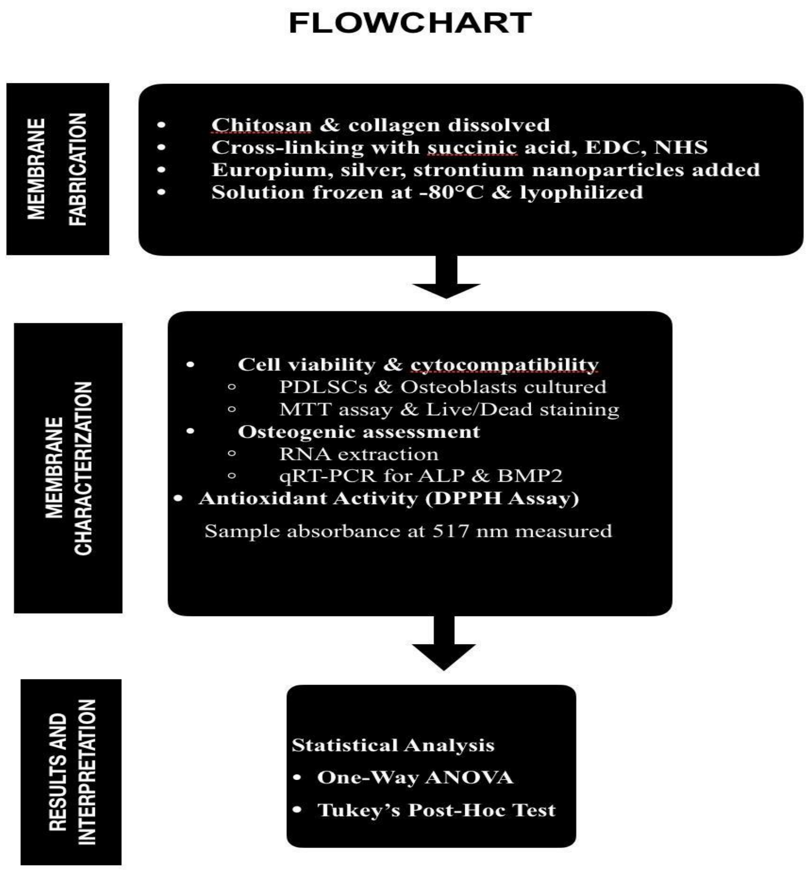

Figure 1. Experimental Flowchart of the study

Antioxidant Activity through DPPH Assay

prepare for the DPPH assay, DPPH was dissolved in ethanol to create a 0.1 mM stock solution, and the solution was protected from light by wrapping it in aluminium foil. Test samples and standard antioxidant (ascorbic acid) solutions were prepared at concentrations of 10, 20, 30, 40, and 50 µg/mL by dilution in ethanol. For the assay, 2.0 mL of the DPPH solution was added to 1.0 mL of each test sample or blank in a test tube. Alternatively, for microplate analysis, 200 µL of DPPH solution was mixed with 100 µL of the sample in each well. All mixtures were incubated at room temperature for 30 min in the dark. After incubation, absorbance was measured at 517 nm using a UV-Vis spectrophotometer, with ethanol used as the blank. A control containing only DPPH and ethanol (no test sample) was included to establish baseline absorbance. Ascorbic acid was used as a reference standard antioxidant for comparison.[27]
Human PDLSCs or osteoblasts were cultured in Dulbecco's Modified Eagle Medium (DMEM) supplemented with 10% foetal bovine serum (FBS) and 1% penicillin–streptomycin. The cells were maintained at 37°C in a humidified atmosphere with 5% CO_2 . For the MTT assay, cells were seeded at a density of 1×10^4 cells/well in a 96-well plate and allowed to adhere for 24 h prior to treatment. The experimental groups included control, Periocol, and europium-doped material. Cells were incubated for 1, 3, and 5 d. At each time point, 10 µL of MTT solution (5 mg/mL in PBS) was added to each well and incubated at 37°C for 4 h. After incubation, 100 µL of DMSO was added to solubilize the formazan crystals, and absorbance was measured at 570 nm using a microplate reader.

To assess cell viability and proliferation, human PDLSCs or osteoblasts were seeded at 1×10^4 cells/well onto the test membranes in 96-well plates. After 24, 72, and 120 h, MTT reagent was added, and absorbance at 570 nm was recorded. For live/dead staining, cells were incubated with calcein-AM and ethidium homodimer-1 for 30 min, and fluorescence microscopy was used to observe viability and attachment at days 1, 3, and 5. To ensure reliability in imaging assessment, two independent observers analysed the fluorescence images, and Cohen's kappa coefficient was calculated to evaluate inter-observer agreement, with values ≥0.80, indicating strong reliability.[28]

Human PDLSCs were cultured in Dulbecco's Modified Eagle Medium (DMEM), and osteoblasts in alpha-Minimal Essential Medium (α-MEM), both supplemented with 10% foetal bovine serum (FBS) and 1% penicillin–streptomycin. The cells were maintained at 37°C in a humidified atmosphere with 5% CO_2 .Cells were seeded at a density of 5×10^4 cells/well in 6-well plates and divided into three experimental groups: Periocol, Eu_2O_3 /Ag_2O/SrO-added collagen–chitosan membrane, and untreated control. Total RNA was extracted on days 1, 7, 14, and 21 using TRIzol reagent (Thermo Fisher Scientific) following the manufacturer's instructions. RNA purity and concentration were assessed using a NanoDrop spectrophotometer (Thermo Fisher Scientific) by measuring 260/280 and 260/230 nm absorbance ratios. One microgram of RNA was reverse transcribed into cDNA using the High-Capacity cDNA Reverse Transcription Kit (Applied Biosystems) according to the protocol.[28]

Quantitative real-time PCR (qRT-PCR) was conducted using the StepOnePlus Real-Time PCR System (Applied Biosystems) and SYBR Green Master Mix (Thermo Fisher Scientific) to quantify relative mRNA levels of BMP-2 and ALP, normalized to β-actin as the internal control. The primer sequences used were as follows:

- BMP-2: Forward: 5′-GCCAGCCGAGCCAACAC-3′, Reverse: 5′-AAATTAAAGAATCTCCGGGTTGT-3′
- ALP: Forward: 5′-GGCAGCGTCAGATGTTAATTG-3′, Reverse: 5′-ACTGCGCTCCTTAGGGCT-3′
- β-actin: Forward: 5′-TCCTGGAGAAGAGCTACG-3′, Reverse: 5′-GTAGTTTCGTGGATGCCACA-3′

Each PCR reaction was performed in a 20 µL mixture containing 2 µL of cDNA, 10 µL of SYBR Green Master Mix, 0.5 µL each of forward and reverse primers, and nuclease-free water. Thermal cycling conditions included an initial denaturation at 95°C for 2 min, followed by 40 cycles of denaturation at 95°C for 15 s, annealing at 60°C for 30 s, and extension at 72°C for 30 s. Gene expression levels were analysed using the $2^{-\Delta\Delta Ct}$ method with normalization to β-actin .[29]

Statistical Analysis

All quantitative data are expressed as mean ± standard deviation (SD) from three independent experiments, each conducted in triplicate. One-way analysis of variance (ANOVA) followed by Tukey's post hoc test was used for multiple group comparisons. A p-value < 0.05 was considered statistically significant.

RESULTS

Surface Morphology and Material Characterization

Scanning Electron Microscopy analysis of the Eu_2O_3 /Ag_2O/SrO-added collagen–chitosan membrane (Figure 2) revealed a rough, multilayered, flake-like surface with an interconnected porous architecture. The incorporation of metal oxides significantly increased surface complexity, mimicking the extracellular matrix and providing a scaffold conducive to cellular behaviors such as attachment, proliferation, and differentiation. The porous and fibrillar network supports nutrient diffusion and cell infiltration, while the rough topography enhances protein adsorption and cell adhesion. Collectively, these morphological features indicate that the modified membrane offers an environment highly favourable for periodontal tissue regeneration.

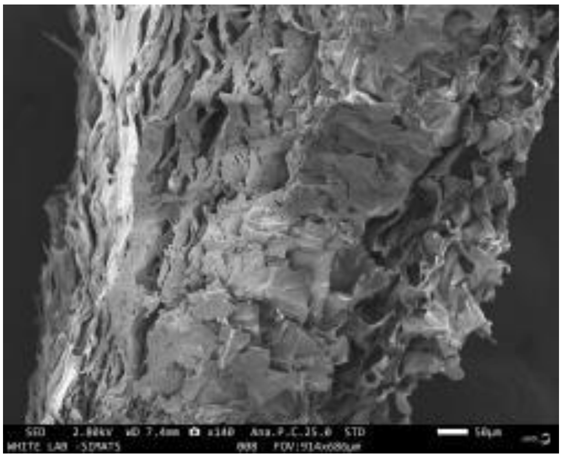

Figure 2. Scanning Electron Micrograph of $Eu_2O_3/Ag_2O/SrO$-Modified Collagen-Chitosan Membrane

Osteogenic Gene Expression Profiles

As shown in Figure 3, ALP mRNA expression, normalized to β-actin, was significantly higher in the Europ+Doped group compared to the Control group at all evaluated time points ($p < 0.05$). Although the Periocol group also exhibited increased ALP expression—particularly on days 14 and 21—the enhancement was less pronounced than in the Europ+Doped group. Notably, no statistically significant differences were observed between groups on day 1, suggesting early-stage parity. However, a progressive, time-dependent increase in ALP expression was observed in the treated groups, peaking at day 14 and remaining elevated through day 21. This trend is further reinforced by the heat map and violin plot visualization (Figure 3), which clearly depicts the distinct gene expression distribution and intensity across groups. These results indicate the Europ+Doped membrane's substantial role in enhancing early osteogenic differentiation.

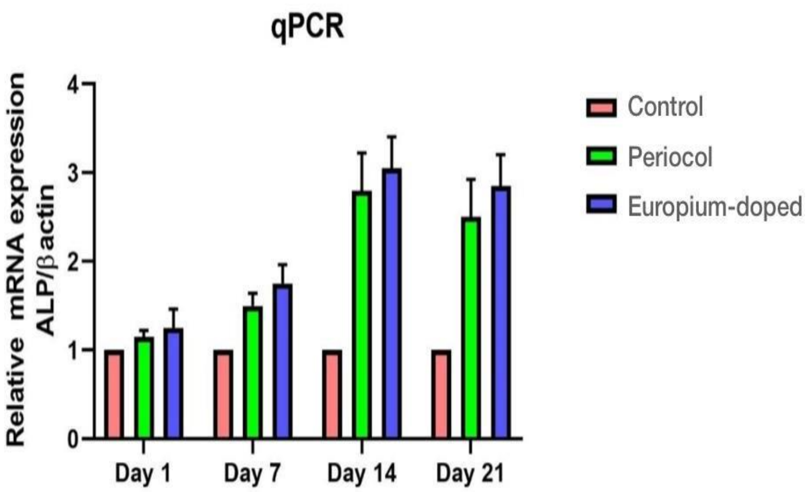

Figure 3 Relative mRNA expression of ALP normalized to β-actin in different experimental groups over time.

Similarly, Figure 4 illustrates BMP-2 mRNA expression trends. The Europ+Doped group demonstrated significantly elevated BMP-2 expression, compared to the Control group at all time points ($p < 0.05$), with the most marked increase seen between days 7 and 21. The Periocol group also showed increased expression, especially on days 7, 14, and 21, but again to a lesser extent than the Europ+Doped scaffold.

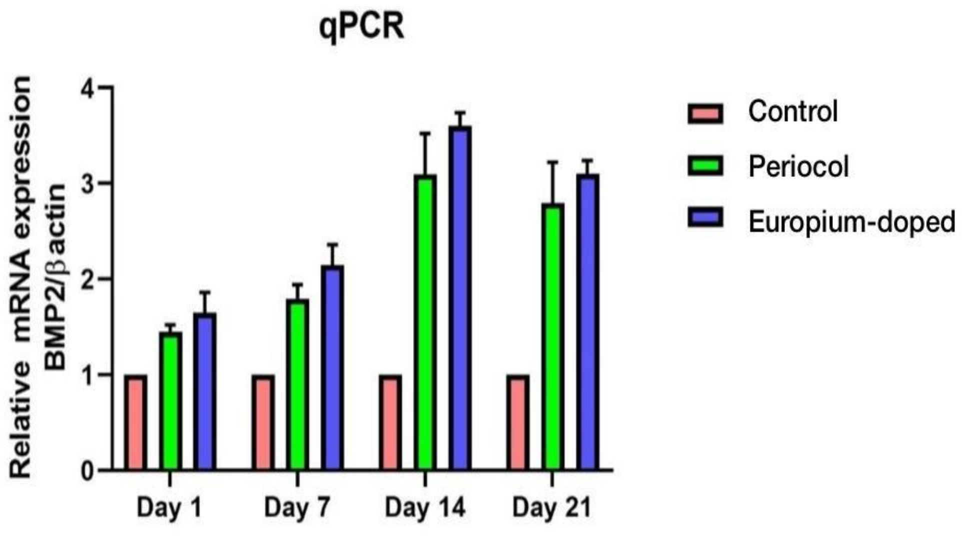

Figure 4. Relative mRNA expression of BMP2 normalized to β-actin in different experimental groups over time.

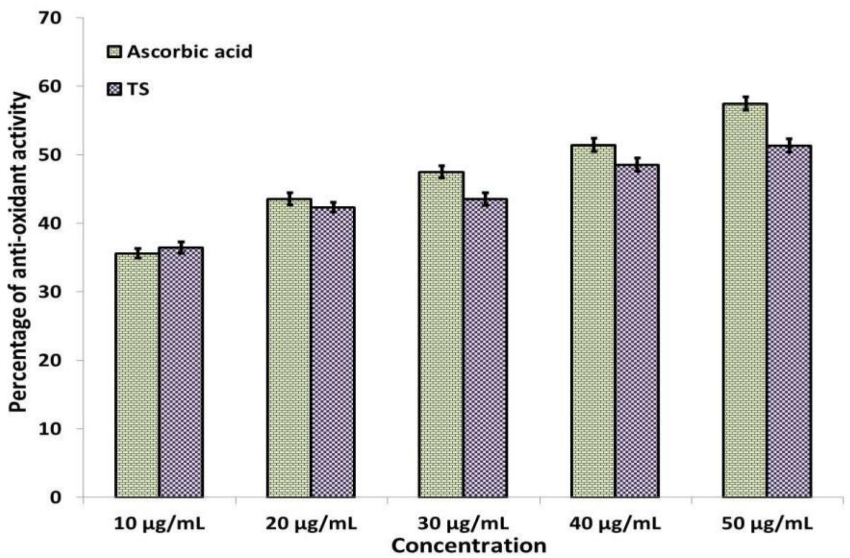

Figure 5. Comparison of Antioxidant Activity Between Ascorbic Acid and Test Sample (Europium-Doped Membrane)

Antioxidant Activity

The antioxidant potential of the europium-doped scaffold (test sample: TS) was comparable to that of standard ascorbic acid, as shown in Figure 5. Both agents displayed a dose-dependent increase in DPPH scavenging activity, starting at approximately 35% at 10 µg/mL and reaching nearly 60% at 50 µg/mL. The comparable antioxidant profiles suggest that the doped membrane can offer oxidative stress mitigation, which is biologically relevant for preventing inflammation-induced bone degradation in regenerative contexts.

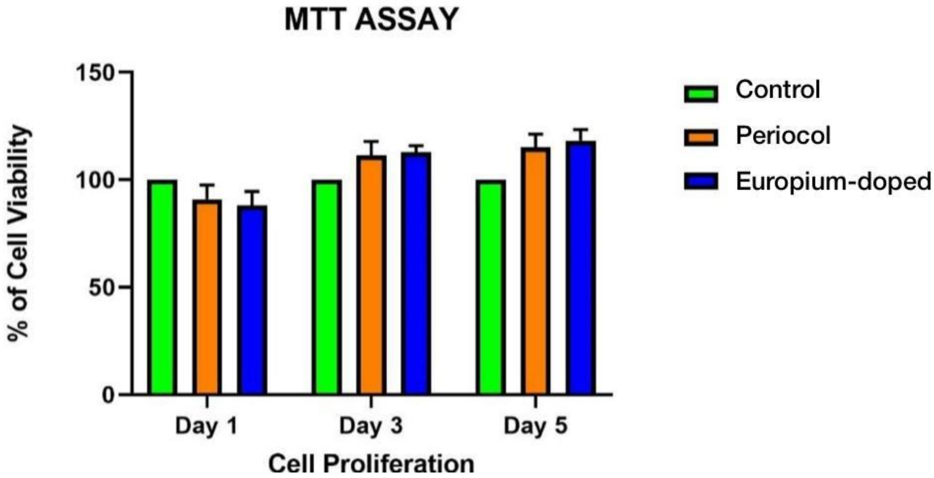

Figure 6. Effect of Control, Periocol, and Europium-Doped Scaffold on Cell Viability over Time as Assessed by MTT Assay

Cytocompatibility and Cell Viability (MTT Assay)

Figure 6 presents the MTT assay–based evaluation of cell viability over days 1, 3, and 5. On day 1, all groups demonstrated comparable viability (~100% in Control, ~95% in Periocol, ~93% in Europium-doped), confirming minimal cytotoxicity at early stages. By day 3, both scaffold groups exhibited enhanced viability (~110% for Periocol and ~112% for Europium-doped), indicating active proliferation. This trend continued on day 5, with the Europium-doped scaffold achieving the highest viability (~120%), surpassing both the Periocol (~118%) and Control (~102%). These results highlight the scaffold's ability to support robust cell proliferation and metabolic activity, both of which are important indicators of in vitro biocompatibility.

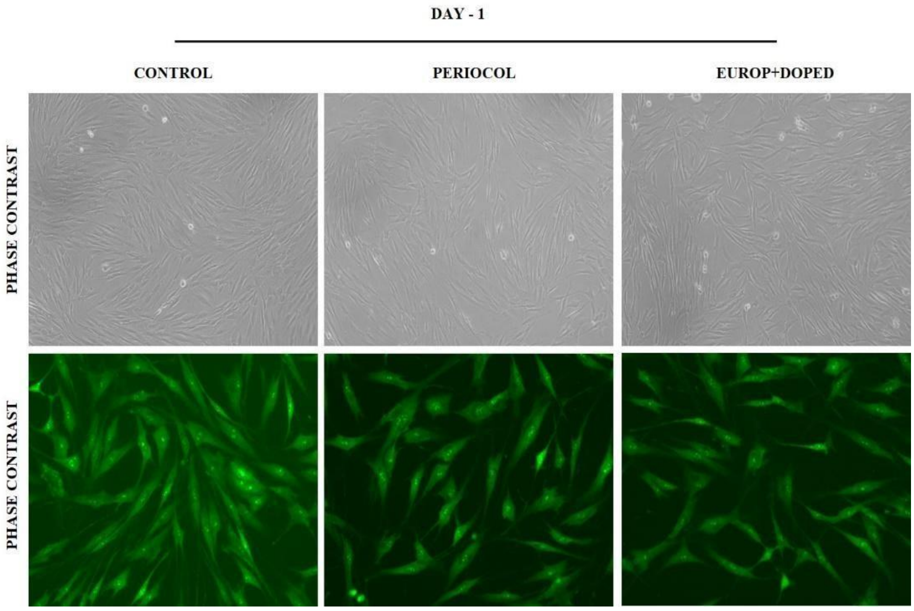

Figure 7a- Phase-Contrast and Fluorescence Microscopy Images of Cells Cultured on Different Scaffolds at Day 1

Cell Morphology and Viability (Fluorescence and Phase-Contrast Imaging)

The scaffold's compatibility was further verified through microscopy imaging on days 1, 3, and 5 (Figures 7a, 7b, and 7c).

- On day 1 (Figure 7a), phase-contrast and fluorescence microscopy revealed well-distributed cells with normal morphology and green fluorescence across all groups, indicating early viability and attachment.
- On day 3 (Figure 7b), both Periocol and Europium-doped scaffolds showed increased cell density and enhanced fluorescence, compared to Control, suggesting accelerated proliferation and favourable microenvironmental interaction.
- On day 5 (Figure 7c), the Europium-doped scaffold displayed the highest confluency and fluorescence intensity, signifying sustained and enhanced cellular growth. These observations are biologically relevant, as they directly reflect the material's ability to support cellular integration, which is a critical factor in scaffold performance for regenerative applications.

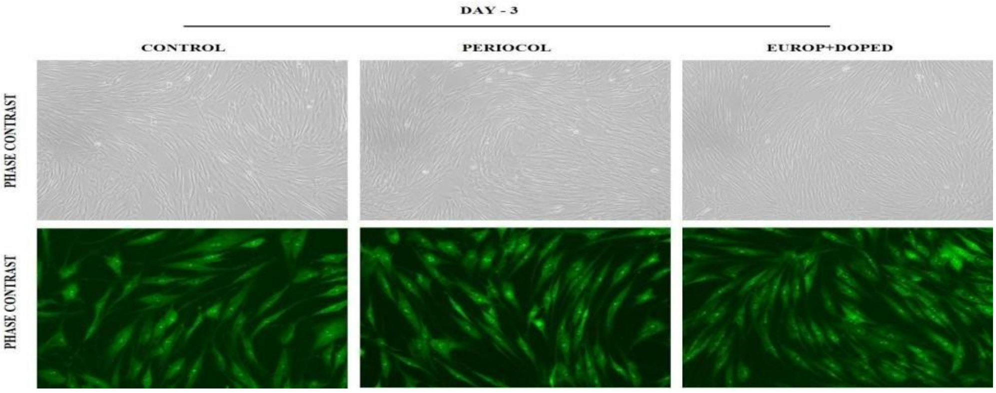

Figure 7b- Phase-Contrast and Fluorescence Microscopy Images of Cells Cultured on Different Scaffolds at Day 3

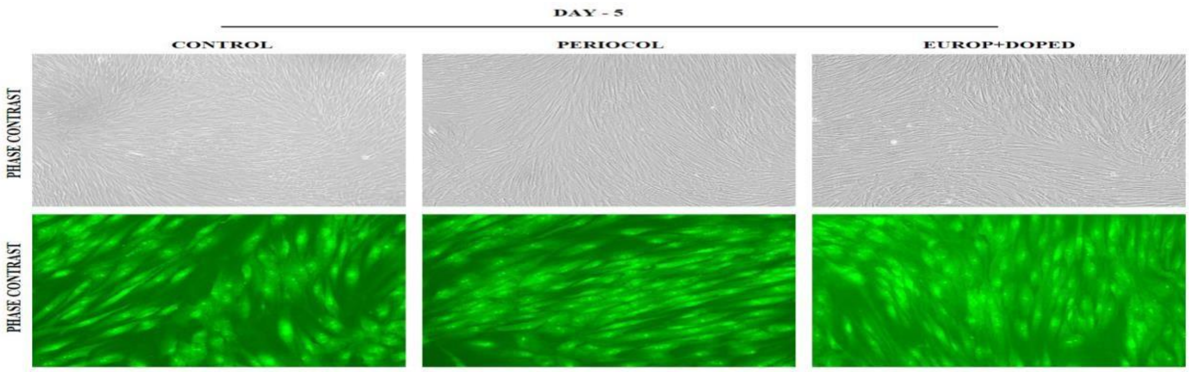

Figure 7c. Phase-Contrast and Fluorescence Microscopy Images of Cells Cultured on Different Scaffolds at Day 5

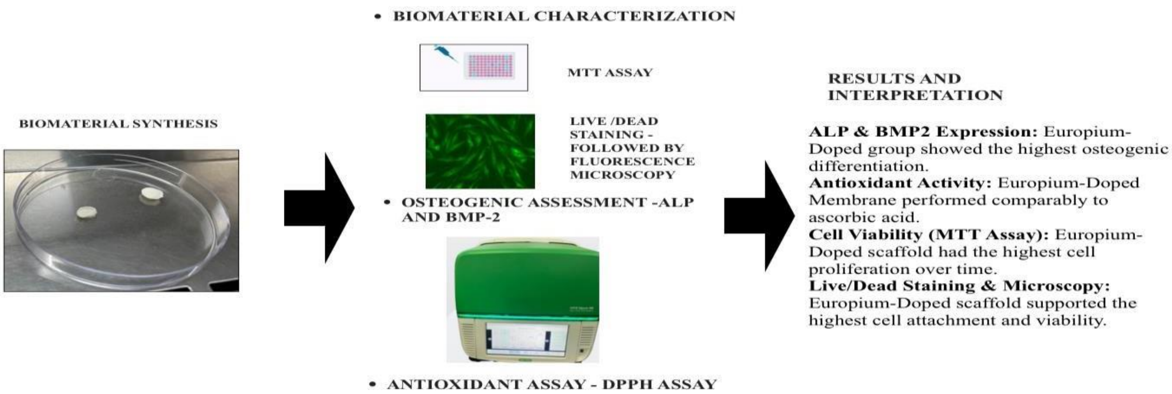

Figure 8. Graphical Abstract: Biomaterial Synthesis, Experimental Workflow, and Key Findings

Figure 8 provides a comprehensive graphical representation of the scaffold synthesis, characterization workflow, and key biological findings. It visually summarizes the interplay between material features and biological outcomes, aiding in translational understanding.

DISCUSSION

The development of a Europium-Strontium-Silver-doped Collagen-Chitosan membrane for guided tissue regeneration (GTR) represents a noteworthy advancement in periodontal therapy by addressing both biological and antimicrobial needs. In this study, a novel europium-silver-strontium-doped collagen-chitosan membrane was evaluated for its antioxidant activity, cytocompatibility, and osteogenic potential using human periodontal ligament cells (hPDLCs) and osteoblasts, with the commercially available PerioCol GTR membrane serving as a control.

Collagen-chitosan composites are well-regarded in GTR applications due to their synergistic biological properties. Collagen facilitates cell adhesion and proliferation owing to its inherent biocompatibility, while chitosan contributes antibacterial effects and improves mechanical characteristics. Together, these components offer a resorbable scaffold supportive of osteogenesis and angiogenesis, and capable of controlled drug delivery.[30] Their combined use enhances membrane stability and resorption kinetics, making them suitable for periodontal and bone tissue regeneration .[31]

The europium-doped membrane exhibited enhanced cell viability and osteogenic response compared to PerioCol. While strontium-doped biomaterials are recognized for promoting osteogenesis, they often exhibit suboptimal antibacterial and mechanical characteristics. To counter these drawbacks, silver was introduced for its well-documented antimicrobial effects, though with the necessary caution regarding dose-dependent cytotoxicity. As demonstrated in prior studies, materials such as graphene oxide or silk fibroin-chitosan gels have been shown to mitigate Ag-related toxicity and further boost both mechanical strength and osteogenesis.[32-34]

The incorporation of Sr and Ag into the europium-doped membrane yielded multifunctional outcomes, combining effective antimicrobial activity with minimal cytotoxicity—evidenced by MTT assays at Days 1, 3, and 5, and Live/Dead staining. Europium's known antimicrobial mechanisms, including ROS generation and membrane disruption[22], further contributed to this synergistic effect.[34]

Additionally, strontium's well-established role in enhancing osteogenesis and angiogenesis[35,36] is reflected in this study's upregulation of ALP and BMP-2, consistent with findings from Zhang J et al. on Sr-based scaffolds.[37] The observed synergy between europium and strontium may account for the improved cell viability and early osteogenic differentiation, aligning with results from Hassani et al.[38] Morphologically, SEM confirmed superior cell spreading and attachment on the doped membrane, indicating favorable conditions for initial tissue integration.

Compared with the PerioCol membrane, the $Eu_2O_3/Ag_2O/SrO$- doped variant displayed superior outcomes across cytocompatibility and osteogenesis. MTT assays consistently showed higher viability at all observed timepoints. Live/Dead staining indicated a greater density of viable cells on the doped membrane. Furthermore, ALP activity and gene expression analysis of ALP and BMP-2 were significantly elevated, supporting the membranes enhanced osteoinductive potential. Antimicrobial testing revealed a broader spectrum of activity, likely due to combined Ag and Eu effects. SEM further demonstrated enhanced cellular interactions with the experimental membrane, underscoring its improved regenerative capability.

The multifunctionality of europium in this context is notable. In addition to its osteogenic influence via ALP upregulation and matrix mineralization [39], it also modulates oxidative stress and inflammation, both of which are critical in the bone healing cascade. Europium-doped calcium polyphosphate scaffolds at 5% concentration—similar to those used in this study—have been shown to stimulate ALP, osteopontin, VEGF, and MMP-9, enhancing angiogenesis and suppressing resorption via OPG/RANKL modulation. Europium-Monetite composites and Eu-doped scaffolds synthesized with eco-friendly techniques have further substantiated its osteogenic benefits, demonstrating improved calcium deposition and collagen synthesis.[21] Recent investigations into 3D EuCPP scaffolds reinforce these observations, particularly those using a 5% europium concentration. These scaffolds supported critical phases of bone regeneration—namely inflammation, proliferation, and remodeling—by enhancing the migration, proliferation, and angiogenic behavior of stromal cells. Upregulation of the OPG/RANKL ratio and osteogenic markers including ALP and osteopontin (OPN) validated the long-term regenerative potential of these materials.[40]Europium's fluorescent properties also introduce an imaging advantage for in vivo scaffold tracking, thereby offering a dual diagnostic and therapeutic role. This feature, while promising, has not been explored in the present study and warrants further investigation. Despite these encouraging findings, several limitations must be acknowledged. This study was limited to in vitro conditions, which do not fully replicate the complexity of in vivo periodontal environments. Moreover, while short-term biological responses were assessed, long-term mechanical stability, enzymatic degradation, and inflammatory responses were not evaluated. The lack of mechanical testing data of the membrane also limits conclusions regarding its functional durability under physiological stress. Additionally, although europium's fluorescence is advantageous for in vivo tracking, it was not applied here and remains a prospective direction. Future studies should therefore explore in vivo models with well-established periodontal defects to confirm biological efficacy and integration. Assessing long-term degradation kinetics, mechanical properties under dynamic load, and host immune responses will be critical for translation. In vivo fluorescence imaging and Kaplan–Meier survival analysis could provide insight into scaffold retention and regenerative longevity. In conclusion, while the $Eu_2O_3/Ag_2O/SrO$-doped collagen-chitosan membrane shows promising in vitro potential for GTR applications—balancing antimicrobial, biocompatible, and osteogenic properties—its translational application must be approached with caution. Further preclinical and clinical evaluations are warranted to substantiate its utility in clinical periodontal regeneration.

CONCLUSION

This study highlights the europium-doped natural polymer-based bio-composite membrane as a promising alternative to the PerioCol GTR membrane. Its combination of mechanical robustness, bioactivity, biocompatibility, and osteogenic potential meets the multifaceted demands of periodontal regeneration. Future in vivo and clinical studies will be essential to further validate its efficacy and pave the way for its adoption in clinical practice.

DECLARATIONS

Competing interest

The authors declare that there are no competing interest.

Funding

The work was not funded.

Ethical Approval

"Not applicable"

Consent for publication

"Not applicable" No funding was received from any financially supporting body

Competing interests

The authors declare no competing interests.

REFERENCES

1. Manakil J. Periodontal Diseases: A Clinician's Guide. BoD – Books on Demand; 2012. 384 p.
2 Dimitriou R, Mataliotakis GI, Calori GM, Giannoudis PV. The role of barrier membranes for guided bone regeneration and restoration of large bone defects: current experimental and clinical evidence. BMC Med. 2012 Jul 26;10:81.
3 Cintra LTA. Guided Tissue Regeneration: Procedures, Health Effects and Long-Term Outcomes. Nova Biomedical Books; 2017.
4 Regeneration of Periodontal Tissues: Guided Tissue Regeneration. Dent Clin North Am. 2010 Jan 1;54(1):73–92.
5 Wang J, Wang L, Zhou Z, Lai H, Xu P, Liao L, et al. Biodegradable polymer membranes applied in guided bone/tissue regeneration: a review. Polymers. 2016 Mar 29;8(4):115.
6 Gottlow J, Nyman S, Karring T, Lindhe J. New attachment formation as the result of controlled tissue regeneration. J Clin Periodontol. 1984 Sep 1;11(8):494–503.
7 Alqahtani AM. Guided tissue and bone regeneration membranes: a review of biomaterials and techniques for periodontal treatments. Polymers. 2023 Aug 10;15(16):3355.
8 Cho YD, Kim KH, Lee YM, Ku Y, Seol YJ. Periodontal wound healing and tissue regeneration: a narrative review. Pharmaceuticals. 2021 May 12;14(5):456.
9 Sasaki JI, Abe GL, Li A, Thongthai P, Tsuboi R, Kohno T, et al. Barrier membranes for tissue regeneration in dentistry. Bioeng Int Dent. 2021 Jan 1;8(1):54–63.
10 Ma YF, Yan XZ. Periodontal guided tissue regeneration membranes: limitations and possible solutions for the bottleneck analysis. Tissue Eng Part B Rev. 2023 Oct 12.
11 Dong C, Lv Y. Application of collagen scaffold in tissue engineering: recent advances and new perspectives. Polymers. 2016 Feb 4;8(2):42.
12 Amirrah IN, Lokanathan Y, Zulkiflee I, Wee MFMR, Motta A, Fauzi MB. A comprehensive review on collagen type I development of biomaterials for tissue engineering: from biosynthesis to bioscaffold. Biomedicines. 2022 Sep 16;10(9):2307.
13 Collagen-based biomaterials for bone tissue engineering. Mater Des. 2021 Nov 15;210:110049.

14 Chitosan as a tool for tissue engineering and rehabilitation: recent developments and future perspectives – a review. Int J Biol Macromol. 2024 Oct 1;278:134172.

15 Chitosan-based bioactive materials in tissue engineering applications – a review. Bioact Mater. 2020 Mar 1;5(1):164–83.

16 Mawazi SM, Kumar M, Ahmad N, Ge Y, Mahmood S. Recent applications of chitosan and its derivatives in antibacterial, anticancer, wound healing, and tissue engineering fields. Polymers. 2024 May 10;16(10):1351.

17 Karthikeyan BS, Madhubala MM, Rajkumar G, Dhivya V, Kishen A, Srinivasan N, et al. Physico-chemical and biological characterization of synthetic and eggshell derived nanohydroxyapatite/carboxymethyl chitosan composites for pulp-dentin tissue engineering. Int J Biol Macromol. 2024 Jun 1;271:132620.

18 Ahmed SF, Ravikumar N, Kavitha S, Mahalaxmi S, Dhivya V, Rajkumar G. Impact of strontium added fluorophosphate glass on the physico-chemical properties of mineral trioxide aggregate. Ceram Int. 2025 Jan 1;51(1):312–9.

19 Dhivya V, Mahalaxmi S, Rajkumar K, Premkumar VV, Saravana Karthikeyan B, et al. Effects of strontium-containing fluorophosphate glasses for enhancing bioactivity and enamel remineralization. Mater Charact. 2021 Nov 1;181:111496.

20 Advanced applications of strontium-containing biomaterials in bone tissue engineering. Mater Today Bio. 2023 Jun 1;20:100636.

21 Suresh N, Kaarthikeyan G. Green synthesis and the evaluation of osteogenic potential of novel europium-doped monetite calcium phosphate by Cissus quadrangularis. Cureus. 2024 Apr;16(4):e59202.

22 Wu L, Yang F, Xue Y, Gu R, Liu H, Xia D, et al. The biological functions of europium-containing biomaterials: a systematic review. Mater Today Bio. 2023 Apr;19:100595.

23 Liu M, Shu M, Yan J, Liu X, Wang R, Hou Z, et al. Luminescent net-like inorganic scaffolds with europium-doped hydroxyapatite for enhanced bone reconstruction. Nanoscale. 2021 Jan 13;13(2):1181–94.

24 Eker F, Duman H, Akdaşçi E, Witkowska AM, Bechelany M, Karav S. Silver nanoparticles in therapeutics and beyond: a review of mechanism insights and applications. Nanomaterials. 2024 Oct 10;14(20):1618.

25 Ran J, Jiang P, Sun G, Ma Z, Hu J, Shen X, et al. Comparisons among Mg, Zn, Sr, and Si doped nano-hydroxyapatite/chitosan composites for load-bearing bone tissue engineering applications. Mater Chem Front. 2017 May 4;1(5):900–10.

26 Baliyan S, Mukherjee R, Priyadarshini A, Vibhuti A, Gupta A, Pandey RP, et al. Determination of antioxidants by DPPH radical scavenging activity and quantitative phytochemical analysis. Molecules. 2022 Feb 16;27(4).

27 Ferreira CMA, Sassone LM, Gonçalves AS, de Carvalho JJ, Tomás-Catalá CJ, García-Bernal D, et al. Physicochemical, cytotoxicity and in vivo biocompatibility of a high-plasticity calcium-silicate based material. Sci Rep. 2019 Mar 8;9(1):1–11.

28 Hosiriluck N, Kashio H, Takada A, Mizuguchi I, Arakawa T. The profiling and analysis of gene expression in human periodontal ligament tissue and fibroblasts. Clin Exp Dent Res. 2022 Jun;8(3):658–72.

29 Bloise N, Petecchia L, Ceccarelli G, Fassina L, Usai C, Bertoglio F, et al. The effect of pulsed electromagnetic field exposure on osteoinduction of human mesenchymal stem cells cultured on nano-TiO2 surfaces. PLoS One. 2018 Jun 14;13(6):e0199046.

30 Ribeiro JCV, Vieira RS, Melo IM, Araújo VMA, Lima V. Versatility of chitosan-based biomaterials and their use as scaffolds for tissue regeneration. Sci World J. 2017 Jan 1;2017:8639898.

31 Guided bone regeneration using chitosan-collagen membranes in dog dehiscence-type defect model. J Oral Maxillofac Surg. 2014 Feb 1;72(2):304.e1–304.e14.

32 Sivolella S, Stellini E, Brunello G, Gardin C, Ferroni L, Bressan E, et al. Silver nanoparticles in alveolar bone surgery devices. J Nanomater. 2012 Jan 1;2012:975842.

33 Liu X, He W, Fang Z, Kienzle A, Feng Q. Influence of silver nanoparticles on osteogenic differentiation of human mesenchymal stem cells. J Biomed Nanotechnol. 2014 Jul;10:7.

34 Physicochemical, osteogenic and antimicrobial properties of graphene oxide reinforced silver/strontium-doped hydroxyapatite on titanium

for potential orthopedic applications. Surf Coat Technol. 2022 Sep 25;446:128788.

35 Li P, Jia Z, Wang Q, Tang P, Wang M, Wang K, et al. A resilient and flexible chitosan/silk cryogel incorporated Ag/Sr co-doped nanoscale hydroxyapatite for osteoinductivity and antibacterial properties. J Mater Chem B. 2018 Nov 21;6(45):7427–38.

36 Hoseinzadeh E, Makhdoumi P, Taha P, Hossini H, Stelling J, Kamal MA, et al. A review on nano-antimicrobials: metal nanoparticles, methods and mechanisms. Curr Drug Metab. 18(2):120–8.

37 Zhang J, Zhu X, Kong Y, Huang Y, Dang X, Mei L, et al. Strontium stimulates alkaline phosphatase and bone morphogenetic protein-4 expression in rat chondrocytes cultured in vitro. J Trace Elem Med Biol. 2019 Sep;55:15–9.

38 Hassani A, Avci ÇB, Kerdar SN, Amini H, Amini M, Ahmadi M, et al. Interaction of alginate with nano-hydroxyapatite-collagen using strontium provides suitable osteogenic platform. J Nanobiotechnol. 2022 Jun 28;20(1):1–22.

39 Fernández-Villa D, Aguilar MR, Rojo L. Europium–tannic acid nanocomplexes devised for bone regeneration under oxidative or inflammatory environments. J Mater Chem B. 2024 Jul 24;12(29):7153–70.

40 Feng S, Peng X, Wu Y, Lei N, Cheng C, Deng Y, Yu X. Europium-doped 3D dimensional porous calcium phosphate scaffolds as a strategy for facilitating the comprehensive regeneration of bone tissue: in vitro and in vivo. ACS Biomater Sci Eng. 2024 Nov 11;10(11):7086–7099